

Supporting Information

β -Sheet Core of Tau Paired Helical Filaments Revealed by Solid-State NMR

Venita Daebel, Subashchandrabose Chinnathambi, Jacek Biernat, Martin Schwalbe, Birgit Habenstein, Antoine Loquet, Elias Akoury, Katharina Tepper, Henrik Müller, Marc Baldus, Christian Griesinger, Markus Zweckstetter, Eckhard Mandelkow, Vinesh Vijayan, and Adam Lange

Material and Methods

Chemicals and Proteins

Heparin (average MW of 5 kDa) and thioflavine S (ThS) were purchased from Sigma-Aldrich (Munich, Germany). Tau constructs of K19 wild type (WT) and K19 mutants were expressed in *E. coli* and purified by heat treatment and FPLC Mono S chromatography GE Healthcare (Freiburg, Germany) as described previously.¹

ssNMR Sample Preparation

WT and mutant K19 proteins were prepared as described previously.¹ The uniform isotopic labeling of K19 protein with ¹⁵N and ¹³C was achieved by expressing K19 in M9 minimal medium containing 1 g liter⁻¹ of ¹⁵NH₄Cl and 4 g liter⁻¹ of ¹³C-glucose. Selectively and extensively labeled protein was obtained by growing bacteria on [2-¹³C] glycerol or [1,3-¹³C] glycerol as described.² The incorporation of natural abundance residues into an otherwise uniformly ¹³C-enriched protein (reverse isotopic labeling) was performed as described.³ Using an analogous method, ¹³C-labeled residues were incorporated into an otherwise natural abundance protein (forward labeling).

PHF Assembly

The aggregation of tau was performed as previously described.⁴ Aggregation was initiated by incubating soluble monomeric tau protein, typically in the concentration range of 50 μ M and in the volume range of 100-150 μ l, in the presence of the anionic cofactor heparin for ~3 days at 310 K. The buffer contained 20 mM BES pH 7.4 and 25 mM NaCl with a K19 protein to heparin ratio of 4:1. The polymerized solution was centrifuged at 40,000 \times g, and the pellet was washed twice with polymerization buffer. The formation of aggregates was monitored by ThS fluorescence and the morphology of filaments was analyzed by electron microscopy.

ThS Fluorescence

PHF formation was monitored by the ThS fluorescence assay as described.⁵ The binding and subsequent increase in ThS fluorescence is specific for the cross- β structure, which is typical for amyloid fibers. 5 μ l of PHF reaction mixture was mixed with 45 μ l of 50 mM NH₄Ac (pH 7) containing 20 μ M ThS. ThS fluorescence was measured in a Tecan spectrofluorimeter (Crailsheim, Germany) with an excitation wavelength of 440 nm and an emission wavelength of 521 nm (slit width 2.5 nm each) in a 384 well plate (black microtiter 384 plate round well; ThermoLab Sys-

tems, Dreieich, Germany). Measurements were carried out at 298 K and the background fluorescence from ThS alone was subtracted. Measurements were carried out in triplicates.

Electron Microscopy

The protein samples were diluted to 1-10 μ M and placed on 600 mesh carbon coated copper grids for 45 seconds, washed twice with H₂O, and negatively stained with 2% uranyl acetate for 45 seconds. The specimens were examined in a Philips CM12 electron microscope at 80 kV.

ssNMR Experiments

We applied two-dimensional ssNMR spectroscopy to assign the resonances of PHF formed by the construct K19. In order to reduce spectral overlap and unambiguously assign the observed residues we investigated not only a uniformly [¹³C, ¹⁵N]-labeled sample (K19_{uni}), but in addition samples with different labeling schemes: 1) a Lys reverse-labeled sample (K19_{Krev}; Lys carbons are unlabeled),^{3,6} 2) a (Lys, Phe, Leu, Val) reverse-labeled sample (K19_{KFLVrev}), 3) a (Cys, Tyr, Leu) forward-labeled sample (K19_{CYLfw}; only Cys, Tyr and Leu carbons are [¹³C]-labeled), 4) a [(1:1)-(¹³C, ¹⁴N: ¹²C, ¹⁵N)]-labeled sample (K19_{1:1})⁷ and 5) glycerol labeled samples (K19_{1,3glyc} and K19_{2glyc}).^{2,8,9}

Furthermore, we studied a uniformly [¹³C, ¹⁵N]-labeled K19 C322A PHF sample. In K19, the mutation of the only cysteine, C322, to an alanine avoids disulfide bond (DSB) formation.

The average ¹³C line-width in the spectra of K19 PHF (Figures 2 and S2) was found to be around 0.5-0.8 ppm. This narrow line-width reflects a higher degree of structural order in the fibrils and much better resolved resonances than seen in previous ssNMR studies on K19 PHF⁴ and may be the result of optimized hydration. Moreover, the spectra of different investigated samples showed an overall similar profile with peaks overlaying well (differences < 0.5 ppm).

¹³C and ¹⁵N chemical shifts were calibrated either with Adamantane as an external reference or with DSS as an internal reference.¹⁰ In the latter case the temperature-dependent position of the water proton resonance was used to measure the temperature inside the MAS rotor.¹¹ Typical proton field strength for 90° pulses and SPINAL-64¹² high-power ¹H-¹³C decoupling was 83 kHz.

For the detection of flexible regions within the protein, ¹³C-¹³C correlation spectra were measured at a spinning frequency of 8.33 kHz using INEPT¹³-based ¹H-¹³C transfer and TOBSY¹⁴-mixing times of 6 ms. For these experiments, GARP¹⁵ decoupling with a field strength of 2.5 kHz was applied on protons.

All other spectra were recorded at a spinning frequency of 11 kHz or in the case of DREAM and PAIN-CP at 18 kHz. An initial ramped cross-polarization (CP) was used to transfer magnetization from ¹H to ¹³C or ¹⁵N with contact times between 700 and 1200 μ s. ¹³C-¹³C transfer was achieved via proton-driven spin-diffusion¹⁶ (PDSD) with mixing times of 20, 150, and 500 ms to obtain intraresidue, sequential, medium- and long-range correlations, respectively. Sequential assignment was also obtained by means of NCACX and NCOCX experiments. ¹⁵N to ¹³C transfer utilized SPECIFIC-CP¹⁷ for a contact time of 2.5-5 ms. In these experiments, PDSD or DREAM¹⁸ elements were used for homonuclear ¹³C-¹³C transfer. Intermolecular ¹⁵N to aliphatic ¹³C transfer was achieved with PAIN-CP¹⁹ and a contact time of 5 ms. The inter-scan delays were set to 2-2.5 s. All NMR spectra were analyzed using Sparky version 3.100 (T. D. Goddard & D.G. Kneller, University of California).

NMR-Detected Solvent Protection of K18 and K19 Filaments

¹⁵N-labeled recombinant K19 and K18 constructs were expressed, purified, and their fibrillation was achieved as previously described. To determine the level of protection from amide proton exchange in the fibrillar state, a previously developed protocol²⁰ was applied. To remove residual monomeric protein and buffer, K18 and K19 filaments were subjected to three consecutive steps of centrifugation for 30 minutes at 25,000 \times g. For forward amide proton exchange, the resulting pellet (8.5 mg K19 and 7.2 mg K18) was then incubated for a total of 36 h in 200 μ l 99.9% D₂O at 278 K. Next, the filaments were pelleted as described above and dissolved in 50% D₂O/50% H₂O, 0.04% formic acid, pH 2.34 and 2 M GuSCN. The backward amide proton exchange was then assessed by a series of two-dimensional ¹H-¹⁵N HSQC spectra recorded at 278 K on Bruker 600 MHz (K19 PHF) and 700 MHz (K18 PHF) NMR spectrometers equipped with a 5 mm triple-resonance, pulsed-field z-gradient cryoprobe. Spectra were recorded with 4 transients and 256 increments in the ¹⁵N dimension, resulting in a total experimental time of 47 or 42 minutes, respectively. The dead time between the dissolution of the PHF and the start of the first experiment was approximately 14 or 10 minutes, respectively. Exchange curves were fitted using IgorPro 5.01. The deuterium incorporation was calculated as described previously.²⁰

For sequential assignment of K18 in the denatured state, three-dimensional TOCSY-HSQC (F1:132 x F2:128 x F3:2K total points) and NOESY-HSQC (F1:144 x F2:144 x F3:2K total points) experiments were acquired in 2 M GuSCN, pH 2.34, 0.04% formic acid, and 50% D₂O/50% H₂O at 700 MHz on a room-temperature 5 mm triple-resonance, pulsed-field z-gradient probe. Together with previously established assignments of K19 and K18²¹ as well

as full-length tau²² in phosphate buffer, the spectra enabled unambiguous assignment of the backbone signals of K18. Taking advantage of the sequence identity of K18 and K19, K19 was assigned based on chemical shift similarities in the HSQC spectra relative to K18. All spectra were processed and analyzed using NMRPipe²³ and CcpNmr Analysis.²⁴

REFERENCES

- (1) Barghorn, S.; Biernat, J.; Mandelkow, E. *Methods Mol Biol* **2005**, 299, 35.
- (2) Castellani, F.; van Rossum, B.; Diehl, A.; Schubert, M.; Rehbein, K.; Oschkinat, H. *Nature* **2002**, 420, 98.
- (3) Vuister, G. W.; Kim, S. J.; Wu, C.; Bax, A. *J Am Chem Soc* **1994**, 116, 9206.
- (4) Andronesi, O. C.; von Bergen, M.; Biernat, J.; Seidel, K.; Griesinger, C.; Mandelkow, E.; Baldus, M. *J Am Chem Soc* **2008**, 130, 5922.
- (5) Friedhoff, P.; Schneider, A.; Mandelkow, E.-M.; Mandelkow, E. *Biochemistry* **1998**, 37, 10223.
- (6) Heise, H.; Hoyer, W.; Becker, S.; Andronesi, O. C.; Riedel, D.; Baldus, M. *Proc Natl Acad Sci USA* **2005**, 102, 15871.
- (7) Etzkorn, M.; Bockmann, A.; Lange, A.; Baldus, M. *J Am Chem Soc* **2004**, 126, 14746.
- (8) LeMaster, D. M.; Kushlan, D. M. *J Am Chem Soc* **1996**, 118, 9255.
- (9) Hong, M. *J Magn Reson* **1999**, 139, 389.
- (10) Morcombe, C. R.; Zilm, K. W. *J Magn Reson* **2003**, 162, 479.
- (11) Bockmann, A.; Gardiennet, C.; Verel, R.; Hunkeler, A.; Loquet, A.; Pintacuda, G.; Emsley, L.; Meier, B. H.; Lesage, A. *J Biomol NMR* **2009**, 45, 319.
- (12) Fung, B. M.; Khitrin, A. K.; Ermolaev, K. *J Magn Reson* **2000**, 142, 97.
- (13) Burum, D. P.; Ernst, R. R. *J Magn Reson (1969)* **1980**, 39, 163.
- (14) Baldus, M.; Meier, B. H. *J Magn Reson, Series A* **1996**, 121, 65.
- (15) Shaka, A. J.; Barker, P. B.; Freeman, R. *J Magn Reson* **1985**, 64, 547.
- (16) Szeverenyi, N. M.; Sullivan, M. J.; Maciel, G. E. *J Magn Reson (1969)* **1982**, 47, 462.
- (17) Baldus, M.; Petkova, A. T.; Herzfeld, J.; Griffin, R. G. *Mol Phys* **1998**, 95, 1197.
- (18) Verel, R.; Baldus, M.; Ernst, M.; Meier, B. H. *Chem Phys Lett* **1998**, 287, 421.
- (19) Lewandowski, J. R.; De Paepe, G.; Griffin, R. G. *J Am Chem Soc* **2007**, 129, 728.
- (20) Cho, M. K.; Kim, H. Y.; Fernandez, C. O.; Becker, S.; Zweckstetter, M. *Protein Sci* **2011**, 20, 387.
- (21) Mukrasch, M. D.; Biernat, J.; von Bergen, M.; Griesinger, C.; Mandelkow, E.; Zweckstetter, M. *J Biol Chem* **2005**, 280, 24978.
- (22) Mukrasch, M. D.; Bibow, S.; Korukottu, J.; Jeganathan, S.; Biernat, J.; Griesinger, C.; Mandelkow, E.; Zweckstetter, M. *PLoS Biol* **2009**, 7, e34.
- (23) Delaglio, F.; Grzesiek, S.; Vuister, G. W.; Zhu, G.; Pfeifer, J.; Bax, A. *J Biomol NMR* **1995**, 6, 277.
- (24) Vranken, W. F.; Boucher, W.; Stevens, T. J.; Fogh, R. H.; Pajon, A.; Llinas, M.; Ulrich, E. L.; Markley, J. L.; Ionides, J.; Laue, E. D. *Proteins* **2005**, 59, 687.

FIGURES

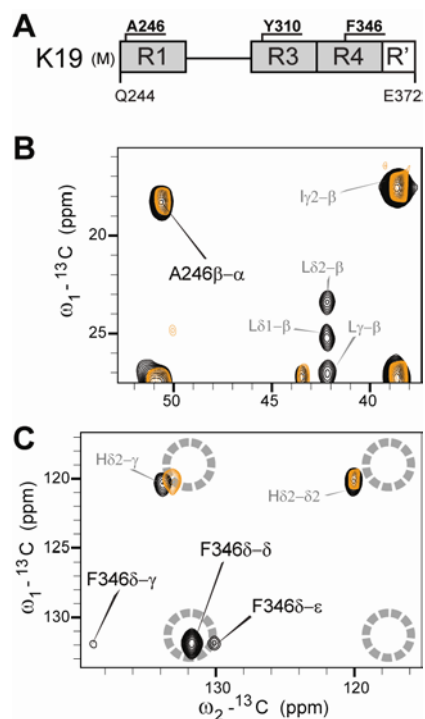


Figure S1. Dynamic segments of K19 PHF. (A) Positions of the three unique residues A246 (in repeat R1), Y310 (in R3), and F346 (in R4). (B, C) Overlay of 2D [^{13}C , ^{13}C]-INEPT-TOBSY ($t_{\text{mix}} = 6$ ms) spectra of K19_{Krev} (black) and K19_{KFLVrev} (orange) PHFs, both acquired on an 850 MHz spectrometer at an MAS rate of 8.333 kHz at 5 °C. (B) An alanine peak is present in the aliphatic region and (C) phenylalanine resonances are visible in the aromatic region of the spectra. The dashed circles indicate positions where tyrosine resonances should appear if Y310 was flexible enough. Notice the absence of phenylalanine resonances in the reverse-labeled K19_{KFLVrev} spectrum, thus validating the F346 assignment. Peaks marked with single letters (e.g., L) were not sequentially assigned.

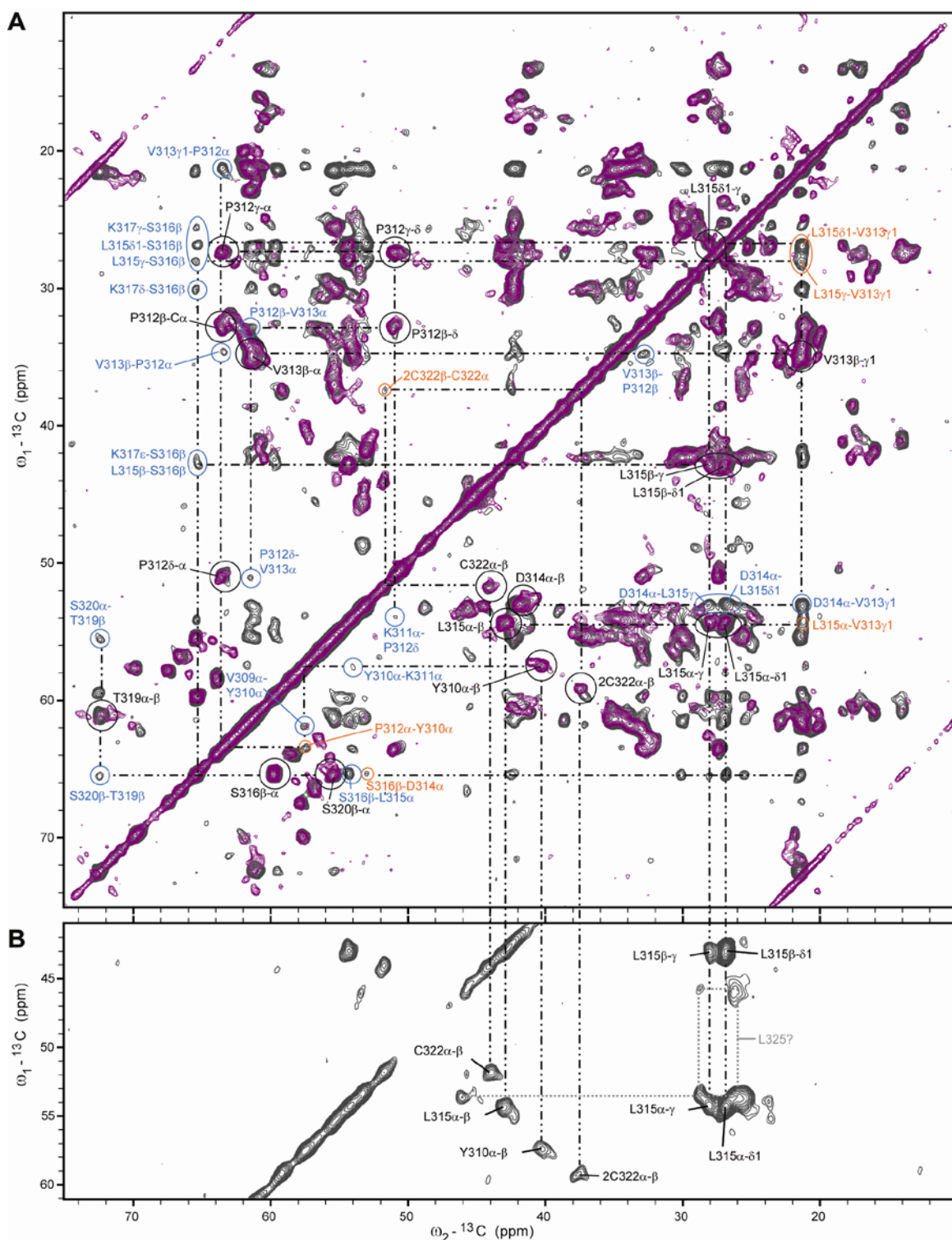


Figure S2. Sequential resonance assignment of the rigid core of K19 PHFs. (A) Overlay of 2D $^{13}\text{C}, ^{13}\text{C}$ -PDSD spectra (black, $t_{\text{mix}} = 150$ ms; purple, $t_{\text{mix}} = 20$ ms) measured on a uniformly $^{13}\text{C}, ^{15}\text{N}$ -labeled K19 PHF sample (K19_{uni}) on an 850 MHz spectrometer at 11 kHz MAS and 7 °C. Intraresidual (black) as well as sequential (blue), and medium- or long-range (orange) connections are highlighted to exemplify the sequential assignment. Resonance assignments for V306 to S324 (in repeat R3) could be obtained. (B) 2D $^{13}\text{C}, ^{13}\text{C}$ -PDSD spectrum ($t_{\text{mix}} = 500$ ms) of a (Cys, Tyr, Leu)- $^{13}\text{C}, ^{15}\text{N}$ forward-labeled sample acquired on a 600 MHz spectrometer at 11 kHz MAS at 7 °C. Noteworthy is the presence of two cysteine resonances, both in an oxidized form (as seen by the chemical shifts), although cysteine is unique in the K19 sequence (C322).

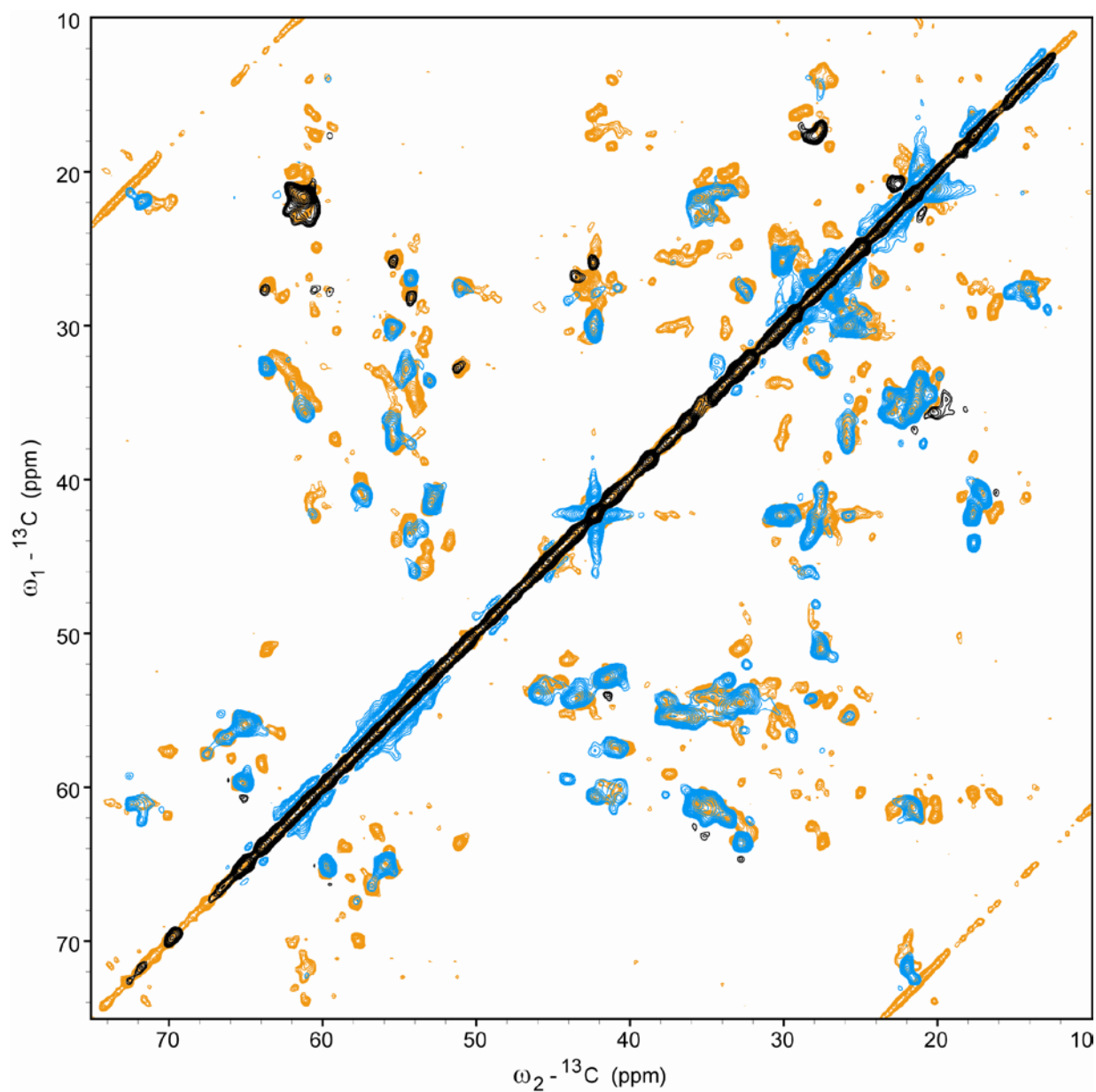


Figure S3. Overlay of PDSD (orange, $t_{\text{mix}} = 20$ ms; recorded on an 850 MHz spectrometer at 11 kHz MAS at 7 °C) and DREAM (black, positive contours; blue, negative contours; $t_{\text{mix}} = 3$ ms; recorded on an 800 MHz spectrometer at 18 kHz MAS at 7 °C) spectra of uniformly [^{13}C , ^{15}N]-labeled K19 PHFs.

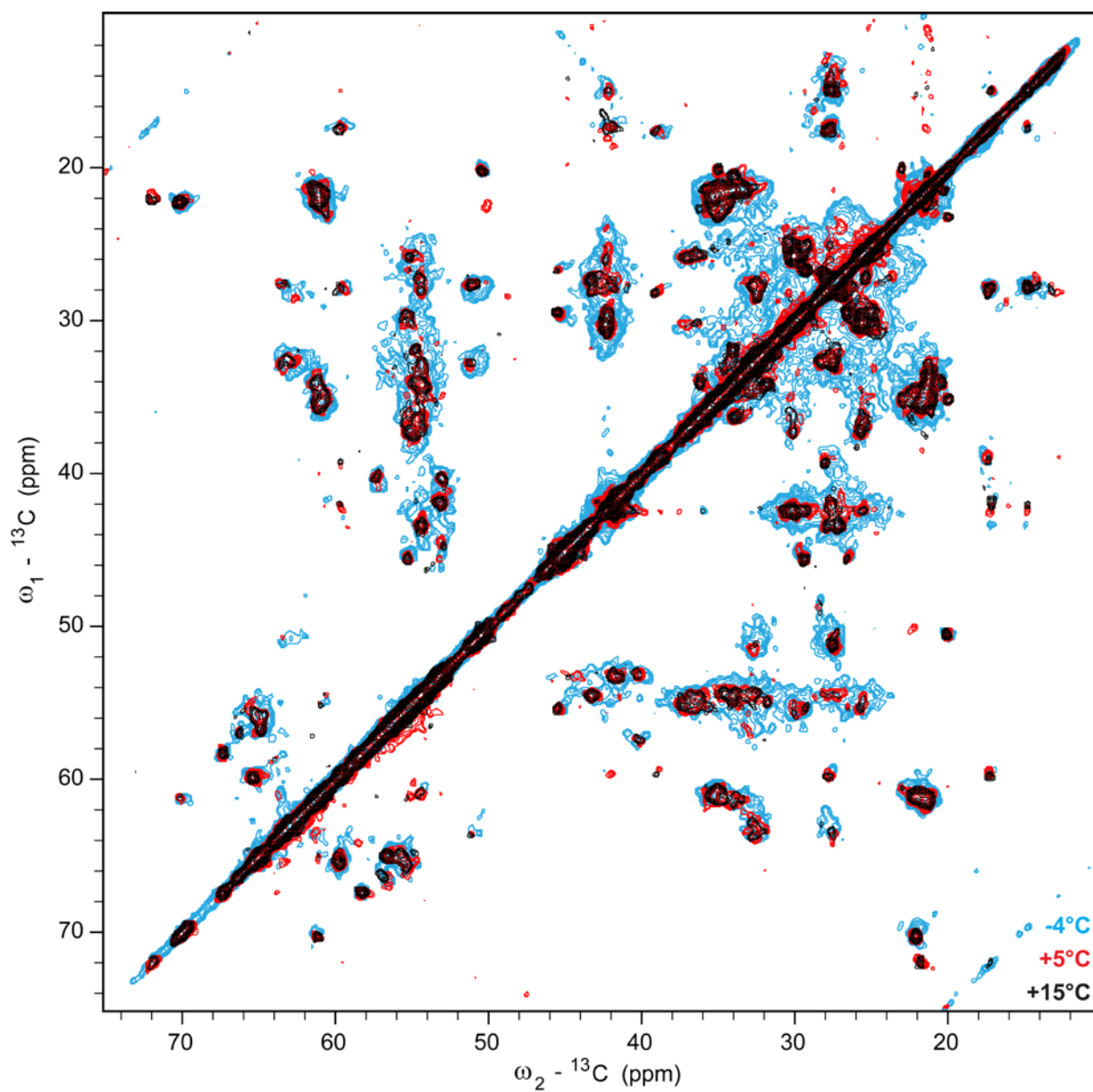


Figure S4. Overlay of PDSD spectra ($t_{\text{mix}} = 20$ ms) of K19C322A PHFs recorded on an 800 MHz spectrometer at 11 kHz MAS at different temperatures (blue, -4°C ; red, 5°C ; black, 15°C).

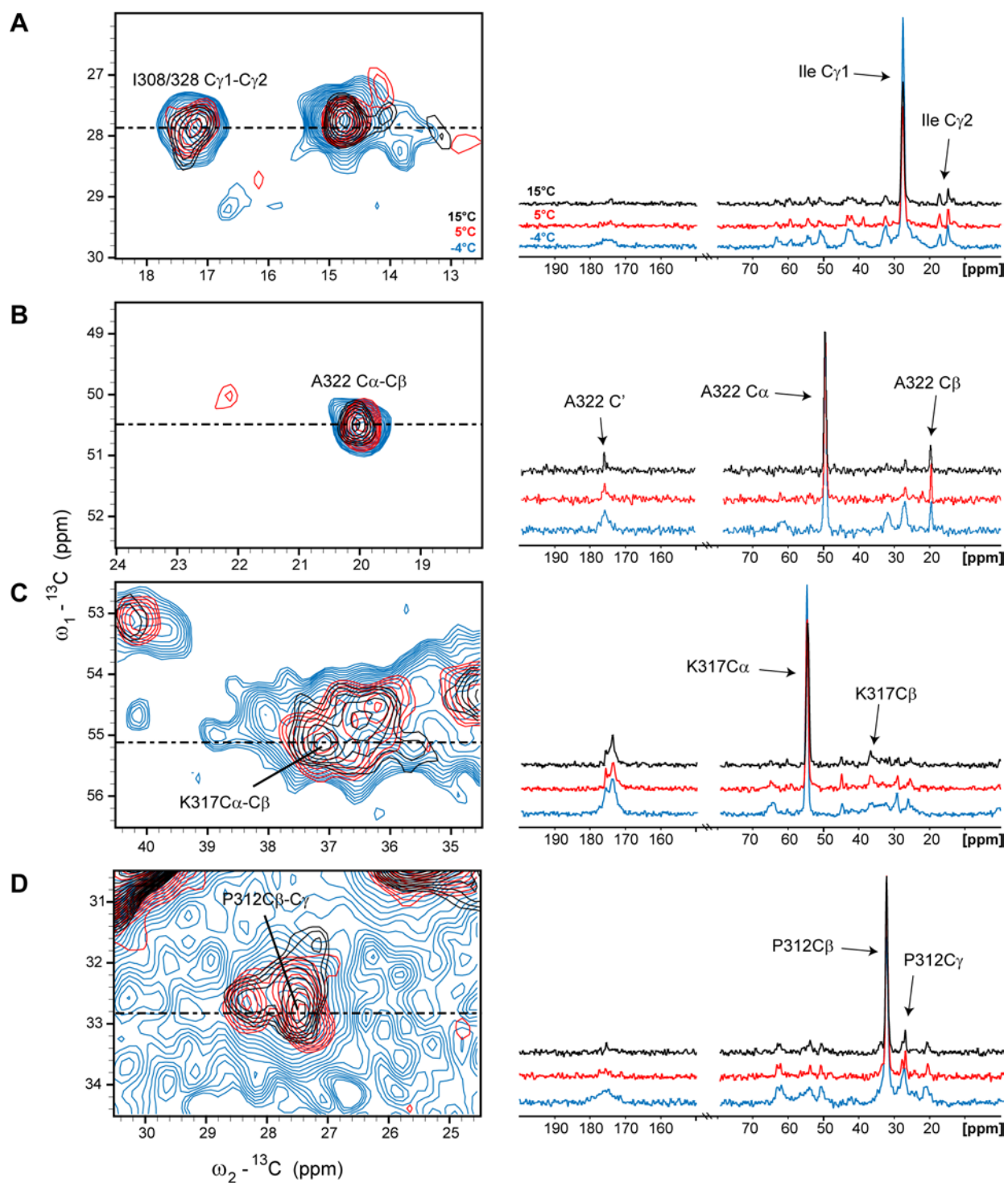


Figure S5. Excerpts from the spectra shown in Figure S4 and 1D traces (PDS spectra ($t_{\text{mix}} = 20$ ms) of K19C322A PHFs recorded on an 800 MHz spectrometer at 11 kHz MAS) exemplifying effects of different temperatures (blue, -4 °C; red, 5 °C; black, 15 °C).

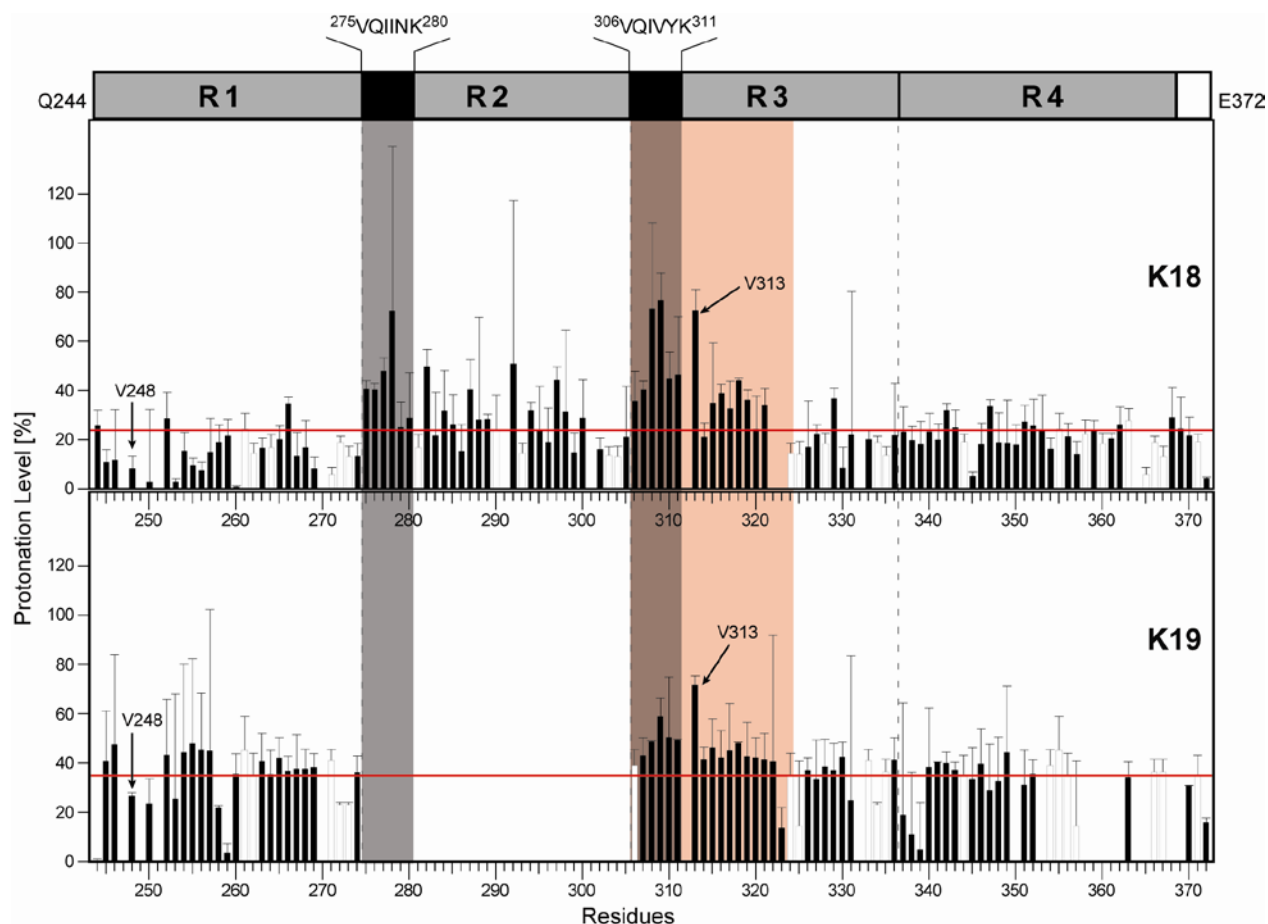


Figure S6. Protonation levels of K18 (upper panel) and K19 (lower panel) filaments after 36 h forward-exchange to D_2O as a function of residue number. Horizontal red lines indicate the average protonation of all residues. Gaps arise from either proline residues or residues that could not be detected. Open bars are averaged values from overlapped residues. On top, the domain orientation of K18 is shown, with the vertical gray bars highlighting the two hexapeptide motifs and the red bar marking the rigid core of K19 PHF. Interestingly, residues identified by the ssNMR study to be within the core region of K19 show the strongest protonation levels in K18 as well, indicating that this region is of central importance also to K18 PHF (unphysical values ($>100\%$) at the y-axis emerge solely from error propagation).

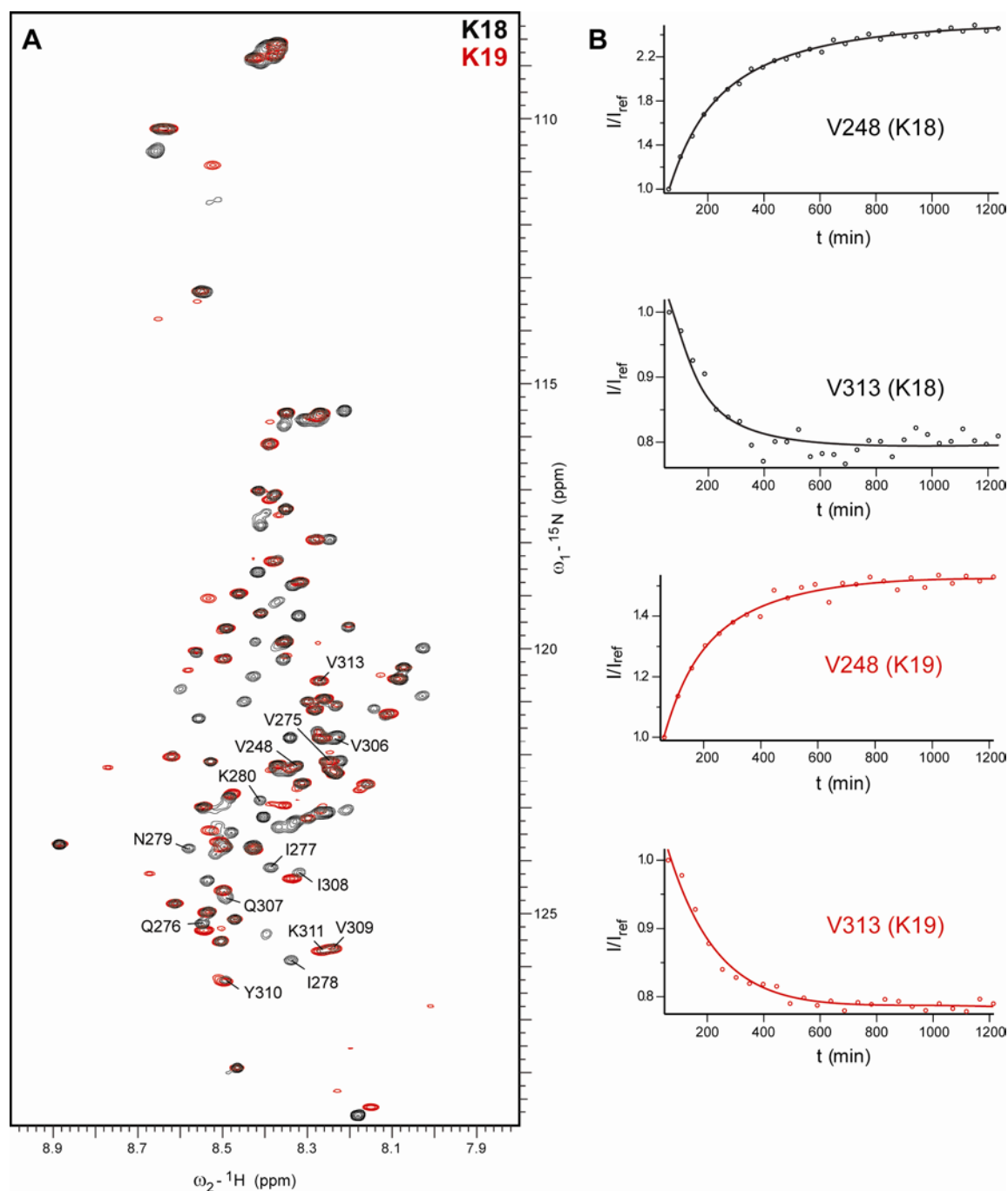


Figure S7. H/D exchange data of K19 and K18. **(A)** Superposition of $[\text{}^1\text{H}, \text{}^{15}\text{N}]$ -HSQC spectra of K18 (black, acquired on a 700 MHz spectrometer at 5°C) and K19 (red, acquired on a 600 MHz spectrometer at 5°C) monomers at 278 K in 2 M GuSCN, 0.04% formic acid, pH 2.34 and 50% $\text{H}_2\text{O}/50\%$ D_2O showing that resonances overlay well. Selected residues, in particular of the two hexapeptide motifs $^{275}\text{VQIINK}^{280}$ (K18) and $^{306}\text{VQIVYK}^{311}$ (K18 and K19), are marked. Note that V306 in K19 and V275 in K18 are surrounded by a similar chemical environment due to the same sequence motif (GKVQI). For this reason, V306 in K19 is shifted with respect to V306 in K18, but overlays well with V275, which itself is not present in K19. **(B)** Time dependence of the HSQC cross-peak intensities of two selected residues, V248 (outside the core region) and V313 (within the core region) of K18 (black) and K19 (red) during backward-exchange are depicted. Intensities are normalized to the intensity of the first spectrum. In both constructs V313 in PHF is protected while V248 is not.

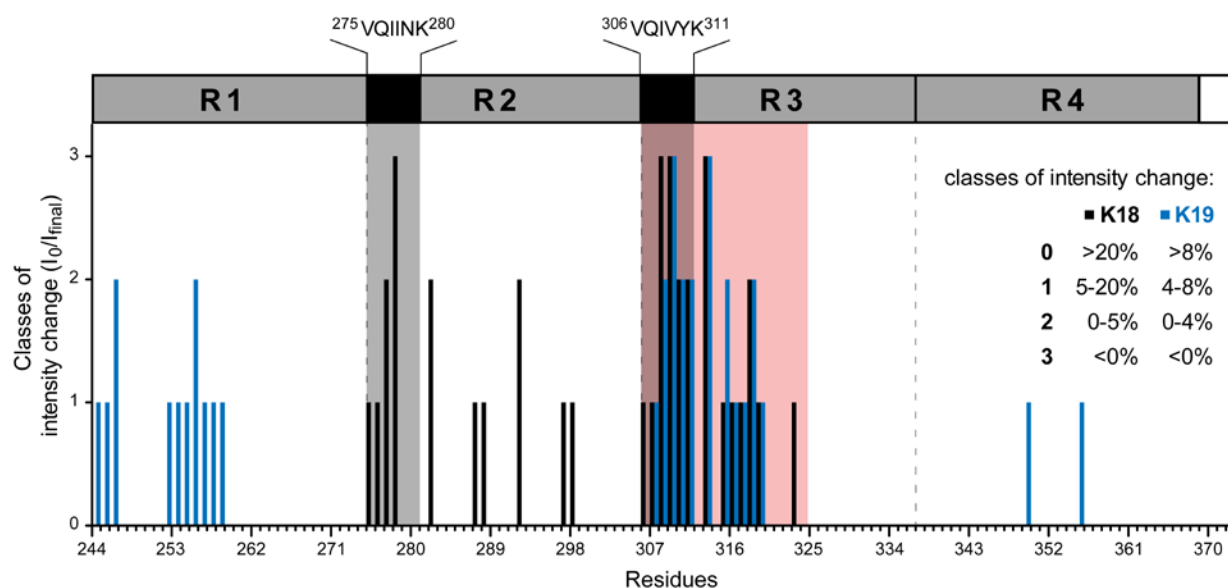


Figure S8. Classification of the HSQC signal intensity change caused by H/D exchange. The percentaged intensity change between the intensity in the first HSQC spectrum and the final intensity (average of the last four HSQC spectra) is classified into four categories for each residue. A signal intensity increase of more than 20% (K18) is scored with a value of zero and is indicative of a solvent exposed residue. In contrast, an intensity decrease indicative of a solvent-protected residue is given a score of three. Residues which are to approximately 50% exchanged to deuterons after forward exchange display hardly any intensity change over time and are scored with two. A fourth class with a score of one is introduced to mark residues, which only show a moderate intensity change compared to stronger exchanging residues. The cut-off values for each class are shown in the inset. The different cut-off values for K18 and K19 result from an overall lower percentaged intensity change for K19. On top, the domain orientation of K18 is shown, with the vertical gray bars highlighting the two hexapeptide motifs and the red bar marking the rigid core of K19 PHF.

TABLES

Table S1. Chemical shift assignment for the rigid core of K19 PHFs. For residues V306–S324, 94% of all backbone and side chain ^{13}C atoms could be assigned.

	N	C	CA	CB	CG/ CG1	CG2	CD/ CD1	CD2	CE/ CE1	CE2	CZ
V306[#]	124.7	-	60.38	35.17	24.99	21.25					
Q307	125.1	174.7	54.05	34.08 [#]	34.78		178.9				
I308	124.8 [#]	174.6	60.52	42.37	29.12	17.7	16.36				
V309	128.3	173.0	61.87	33.81	21.2	20.1					
Y310	132.2	172.9	57.52	40.24	127.7		134.5	133.7	118.8	118.2	157.3
K311	125.2	171.2	54.08	33.05 [#]	24.79		30.53		42.05		
P312	134.8	175.5	63.58	32.85	27.44		51.02				
V313	119.4	174.8	61.42	34.66	21.35 [*]						
D314	128.2	174.1	53.07	41.79	179.5						
L315	129.0	177.1	54.34	42.89	28.0		26.91 [*]				
S316	119.8	174.1	59.78	65.37							
K317	116.4	176.2	55.27	37.09	25.65		30.05		42.36		
V318	127.2	175.5	61.48	35.24 [#]	22.92	21.52					
T319	124.0	172.9	61.08	72.44		21.4					
S320	119.6	173.9	55.5	65.44							
K321	124.4	-	54.1	34.2	-		-		-		
C322	115.3	174.1	51.72	44.08							
G323	111.9	-	45.79								
S324	114.3	173.3	56.8	66.63							
2K321	123.6	174.7	55.79	33.9	25.41		29.91		42.3		
2C322	123.6	173.7	59.17	37.44							
2G323	112.8	-	45.05								
2S324	121.3	173.7	57.88	67.53							

- indicates unassigned resonances.

^{*} indicates C γ 1/C γ 2 or C δ 1/C δ 2 resonances with identical chemical shift.[#] indicates ambiguity